Supporting Information

Separation/Purification of Ethylene from Acetylene/Ethylene Mixture in a Pillared-layer Porous Metal-Organic Framework

Arpan Hazra,[a] Saibal Jana,[a] Satyanarayana Bonakala,[a] Sundaram Balasubramanian[a] and Tapas Kumar Maji*[a]

[a] *Chemistry and Physics of Materials Unit, Jawaharlal Nehru Centre for Advanced Scientific Research, Jakkur, Bangalore, 560 064, India.*

*To whom correspondence should be addressed. T. K. Maji: E-mail: tmaji@jncasr.ac.in; Tel: (+91)-80-2208-2826; Fax: (+91)-80-2208-2766.

Contents

Experimental Section

Materials

All the reagents and solvents employed were commercially available and used as supplied without further purification. $K_3[Mn(CN)_6]$, 4,4′-bipyridine (bipy) and $MnCl_2 \cdot 6H_2O$ were obtained from the Aldrich Chemical Co. All the solvents used during the synthesis were degassed at 50 °C for 12 hr under constant Ar flow. The pretreatment at higher temperature was necessary to remove the dissolved oxygen form the solvents. All preparations were carried out under dark and anaerobic conditions (Ar flow) using standard Schlenk apparatus to avoid oxidation by atmospheric oxygen.

Synthetic procedure

Synthesis of $\{[Mn_3(bipy)_3(H_2O)_4][Mn(CN)_6]_2 \cdot 2(bipy) \cdot 4H_2O\}_n$ (1): $\{[Mn_3(bipy)_3(H_2O)_4][Mn(CN)_6]_2 \cdot 2(bipy) \cdot 4H_2O\}_n$ (**1**): An aqueous solution (12.5 mL) of $K_3[Mn(CN)_6]$ (0.25 mmol) was added to an ethanolic solution (12.5 mL) of bipy (0.5 mmol) and stirred for 30 min. $MnCl_2 \cdot 6H_2O$ (0.25 mmol) was dissolved in 12.5 mL water and 2.5 mL of this metal solution was carefully layered with the 2.5 mL of mixed bipy and $K_3[Mn(CN)_6]$ solution using an ethanol : water buffer solution (1 mL, 1:1) in a test tube. The reaction was performed under completely dark condition and the test tube was kept in a fridge (~4°C) after wrapping with aluminum foil. After 15 days, dark brown block shaped crystals were appeared in the middle of the tube and separated and washed with ethanol. The bulk amount of the sample was prepared in similar reaction condition by the direct mixing of the respective reagents in ethanol-water solution under stirring for 24 h and the phase purity was checked with the PXRD (Fig.S3) and elemental analysis. Yield: 79%, relative to Mn^{II}. Anal. Calc. for $C_{62}H_{56}Mn_5N_{22}O_8$: C, 49.25; H, 3.73; N, 20.38. Found: C, 49.81; H, 3.58; N, 20.18. IR (KBr, cm^{-1}): $\nu(OH)$ 3679, 3585, 3488; $\nu(ArC\text{-}H)$ 3066, 3051; $\nu(C\equiv N)$ 2154, 2131; $\nu(ArC=C)$ 1604, 1560, 1534. IR spectrum of **1**(Fig. S4) shows strong and broad bands around 3490 cm^{-1} suggesting the presence of water molecules. A strong band around 2131 cm^{-1} corroborate to $\nu(C\equiv N)$ stretching frequency and a band around 1604 cm^{-1} indicates the presence bipy molecule.

Preparation of {[Mn$_3$(bipy)$_3$][Mn(CN)$_6$]$_2$}$_n$ (1a): Compound **1a** was prepared by heating compound **1** in QUANTACHROME sample cell at 150 ℃ under a reduced pressure ($< 10^{-1}$ Pa) for 72 hrs. During the heating, the sublimed guest bipy molecules were deposited on the upper inner part of the adsorption cell (Fig. S2). The heating procedure was continued following with the change of the sample cells unless there was no tress of sublimated guest bipy molecule. The removal of the water molecules (coordinated and guest) was confirmed by the elemental analysis. This powdered sample was used for characterization of different physical properties. Anal. Calc. for C$_{42}$H$_{24}$Mn$_5$N$_{18}$: C, 47.80; H, 2.29; N, 23.89. Found: C, 47.09; H, 2.41; N, 23.45.

Preparation of {[Mn$_3$(bipy)$_3$(H$_2$O)$_2$][Mn(CN)$_6$]$_2$·2(bipy)·2H$_2$O}$_n$ (1b): Single crystal of Compound **1** was heated at 135 ℃ with a flow of dry air in a goniometer of Bruker D8 VENTURE single crystal X-ray diffractometer. Structural determination reveals that, we were able to remove two of each guest and coordinated water molecules (total 4 water molecules/formula unit) from compound **1** to yield **1b**.

Physical Measurements

The elemental analyses of each compound and their corresponding dehydrated phases were carried out on a Thermo Fisher Flash 2000 Elemental Analyser. Fourier transformed IR spectroscopic studies were carried out using a KBr pellet (Bruker IFS-66v). Thermogravimetric analysis (TGA) was carried out (Mettler Toledo) in N$_2$ atmosphere (flow rate = 50 ml min^{-1}) in the temperature range 30 – 700 °C (heating rate = 2°C min^{-1}). Powder XRD pattern of the products were recorded by using Cu-K_α radiation (Bruker D8 Discover; 40 kV, 30 mA).

Single Crystal X-ray Diffraction

Suitable single crystal of compound **1** was mounted on a thin glass fiber with commercially available super glue. X-ray single crystal structural data of **1** was collected on a Bruker Smart-CCD diffractometer equipped with a normal focus, 2.4 kW sealed tube X-ray

source with graphite monochromated Mo-Kα radiation (λ = 0.71073 Å) operating at 50 kV and 30 mA.The partially solvent removed structure of compound **1** (*i.e.* compound **1b**) was collected on a Bruker D8 VENTURE with Mo-Kα radiation (λ = 0.71073 Å) operating at 50 kV and 1 mA. The program SAINT[1] was used for the integration of diffraction profiles and absorption correction was made with SADABS[2] program. All the structures were solved by SIR 92[3] and refined by full matrix least square method using SHELXL.[4] All the hydrogen atoms were fixed by HFIX and placed in ideal positions. Potential solvent accessible area or void space was calculated using the PLATON[5] multipurpose crystallographic software. All crystallographic, structure refinement data and bond distance and angles of **1** and **1b** are summarized in Table S1-S5. All calculations were carried out using SHELXL 97,[4] PLATON,[5] SHELXS 97 [4] and WinGX system, Ver 1.80.05.[6]

Table S1: Crystallographic Data and Structure Refinement Parameters for Compounds **1** and **1b**.

	1	1b
Empirical formula	$C_{62}H_{56}Mn_5N_{22}O_8$	$C_{62}H_{48}Mn_5N_{22}O_4$
M	1511.99	1439.92
Crystal system	Orthorhombic	Orthorhombic
space group	*Pbam* (No. 55)	*Pbam* (No. 55)
a (Å)	16.2079(18)	16.039(5)
b (Å)	17.833(2)	17.851(4)
c (Å)	11.6508(12)	11.558(3)
α(deg)	90	90
β (deg)	90	90
γ (deg)	90	90
V (Å^3)	3367.5(6)	3309.2(15)
Z	2	2
T(K)	296	408
λ(Mo K$_\alpha$)	0.71073	0.71073
D_c (g cm^{-3})	1.491	1.445
μ (mm^{-1})	0.982	0.991
$\theta_{max}/\theta_{min}$ (deg)	28.3/2.9	25.0/2.3

total data	56112	18701
unique reflection	4394	3018
R_{int}	0.061	0.109
data [$I > 2\sigma(I)$]	3331	1400
R[a]	0.0433	0.1098
R_w[b]	0.1350	0.2883
GOF	1.04	0.94
$\Delta\rho$ min/max [e Å⁻³]	-0.57, 0.81	-0.72, 0.74

[a]$R = \sum||Fo|-|Fc||/\sum|Fo|$; [b]$R_w = [\sum\{w(Fo^2-Fc^2)^2\}/\sum\{w(Fo^2)^2\}]^{1/2}$

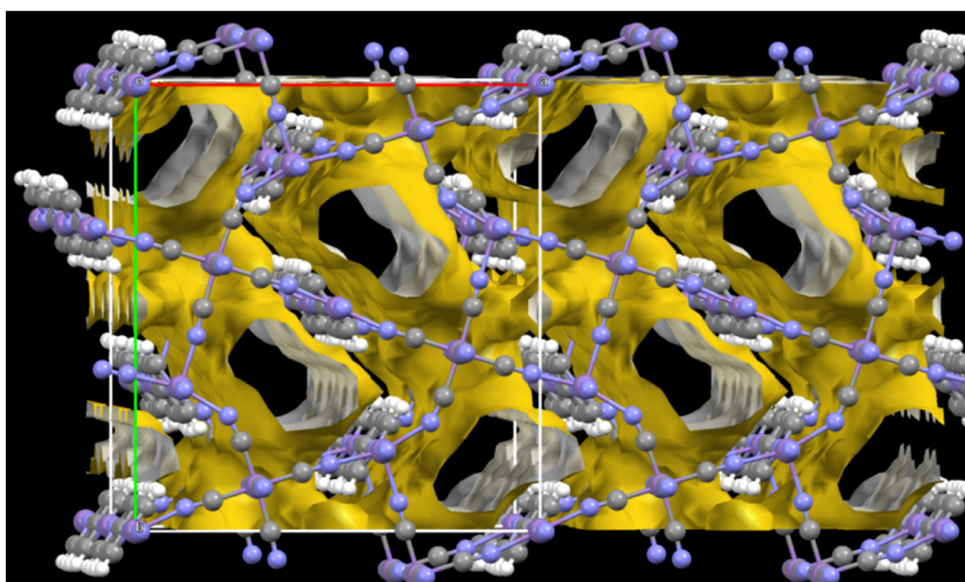*Fig. S1:* Connolly surface of the 1D channel along the *c* direction present in compound **1**.

Fig. S2: Guest 4,4′-bipy of compound **1** was removed during the activation procedure which was deposited in the inner wall of adsorption cell.

Table S2: Selected bond lengths in compound **1**.

Bonds	Bond length (Å)	Bonds	Bond length (Å)
Mn1−C1	1.882(3)	Mn1−C2	1.887(3)
Mn1−C3	1.917(2)	Mn1−C4	1.892(3)
Mn1−C5	1.877(3)	Mn1−C3_h	1.917(2)
Mn2−O2W	2.259(2)	Mn2−N5	2.185(3)
Mn2−N6	2.270(2)	Mn2−O2W_a	2.259(2)
Mn2−N5_a	2.185(3)	Mn2−N6_f	2.270(2)
Mn3−O1W	2.204(3)	Mn3−N4	2.229(3)
Mn3−N7	2.274(2)	Mn3−N1_c	2.193(3)
Mn3−N2_d	2.148(3)	Mn3−N7_h	2.274(2)

Table S3: Selected bond angles in compound **1**.

	Angles(º)		Angles(º)
C1−Mn1−C2	90.48(14)	O2W_a−Mn2−N6_f	90.00
C1−Mn1−C3	89.80(7)	N5_a−Mn2−N6_f	90.00
C1−Mn1−C4	92.64(14)	O1W−Mn3−N4	80.93(11)
C1−Mn1−C5	179.31(14)	O1W−Mn3−N7	88.10(6)
C1−Mn1−C3_h	89.80(7)	O1W−Mn3−N1_c	82.02(11)
C2−Mn1−C3	89.84(7)	O1W−Mn3−N2_d	175.52(12)
C2−Mn1−C4	176.88(13)	O1W−Mn3−N7_h	88.10(6)
C2−Mn1−C5	88.83(14)	N4−Mn3−N7	90.48(6)
C2−Mn1−C3_h	89.84(7)	N1_c−Mn3−N4	162.95(11)
C3−Mn1−C4	90.17(7)	N2_d−Mn3−N4	103.56(11)
C3−Mn1−C5	90.20(7)	N4−Mn3−N7_h	90.48(6)
C3−Mn1−C3_h	179.49(11)	N1_c−Mn3−N7	88.96(6)
C4−Mn1−C5	88.05(14)	N2_d−Mn3−N7	91.83(6)
C3_h−Mn1−C4	90.17(7)	N7−Mn3−N7_h	175.89(9)
C3_h−Mn1−C5	90.20(7)	N1_c−Mn3−N2_d	93.50(12)
O2W−Mn2−N5	85.12(10)	N1_c−Mn3−N7_h	88.96(6)

O2W−Mn2−N6	90.00	N2_d−Mn3−N7_h	91.83(6)
O2W−Mn2−O2W_a	180.00	O2W−Mn2−N5_a	94.88(10)
O2W−Mn2−N6_f	90.00	O2W_a−Mn2−N5_a	85.12(10)
N5−Mn2−N6	90.00	Mn2−N6−C6_a	122.26(14)
O2W_a−Mn2−N5	94.88(10)	Mn2−N5−C5	170.2(3)
N5−Mn2−N5_a	180.00	Mn3−N4−C4	148.4(3)
N5−Mn2−N6_f	90.00	O2W_a−Mn2−N6	90.00
N5_a−Mn2−N6	90.00	Mn3_b−N1−C1	177.6(3)
N6−Mn2−N6_f	180.00	Mn3_e−N2−C2	175.9(3)

a = 1−x,1−y,z; c =1/2+x,1/2−y,2−z; d =1/2−x,−1/2+y,2−z; f =1−x,1−y,2−z; h =x,y,2−z

Table S4: Selected bond lengths in compound **1b**.

Bonds	Bond length (Å)	Bonds	Bondlength (Å)
Mn1−C1	2.005(11)	Mn1−C2	2.037(10)
Mn1−C3	2.041(8)	Mn1−C4	2.029(12)
Mn1−C5	2.002(12)	Mn1−C3_h	2.041(8)
Mn2−O2W	2.222(11)	Mn2−N5	2.121(12)
Mn2−N6	2.270(9)	Mn2−O2W_a	2.222(11)
Mn2−N5_a	2.121(12)	Mn2−N6_f	2.270(9)
Mn3−N4	2.024(12)	Mn3−N7	2.269(7)
Mn3−N1_c	2.049(11)	Mn3−N2_d	2.037(11)
Mn3−N7_h	2.269(7)		

Table S5: Selected bond angles in compound **1b**.

	Angles (º)		Angles (º)
C1−Mn1−C2	93.1(5)	O2W_a−Mn2−N6_f	90.00
C1−Mn1−C3	89.9(3)	N5_a−Mn2−N6_f	90.00
C1−Mn1−C4	91.7(4)	N4−Mn3−N7	89.6(2)
C1−Mn1−C5	177.7(5)	N1_c−Mn3−N4	139.6(5)

C1−Mn1−C3_h	89.9(3)	N2_d−Mn3−N4	115.8(5)
C2−Mn1−C3	89.5(3)	N4−Mn3−N7_h	89.6(2)
C2−Mn1−C4	175.3(5)	N1_c−Mn3−N7	87.2(2)
C2−Mn1−C5	89.2(5)	N2_d−Mn3−N7	94.43(18)
C2−Mn1−C3_h	89.5(3)	N7−Mn3−N7_h	170.5(3)
C3−Mn1−C4	90.6(3)	N1_c−Mn3−N2_d	104.6(5)
C3−Mn1−C5	90.1(3)	N1_c−Mn3−N7_h	87.2(2)
C3−Mn1−C3_h	178.9(4)	N2_d−Mn3−N7_h	94.43(18)
C4−Mn1−C5	86.1(5)	Mn3_b−N1−C1	152.0(10)
C3_h−Mn1−C4	90.6(3)	Mn3_e−N2−C2	168.1(13)
C3_h−Mn1−C5	90.1(3)	Mn1−C2−N2	177.4(12)
O2W−Mn2−N5	86.3(5)	Mn1−C3−N3	174.8(10)
O2W−Mn2−N6	90.00	O2W_a−Mn2−N5_a	86.3(5)
O2W−Mn2−O2W_a	180.00	Mn3−N4−C4	160.3(11)
O2W−Mn2−N5_a	93.7(5)	Mn2−N5−C5	169.9(14)
O2W−Mn2−N6_f	90.00	Mn2−N6−C6	121.7(5)
N5−Mn2−N6	90.00	Mn2−N6−C6_a	121.7(5)
O2W_a−Mn2−N5	93.7(5)	Mn1−C4−N4	170.2(10)
N5−Mn2−N5_a	180.00	Mn3−N7−C13	124.1(6)
N5−Mn2−N6_f	90.00	Mn3−N7−C9	121.4(8)
O2W_a−Mn2−N6	90.00	N5_a−Mn2−N6	90.00
Mn1−C1−N1	179.0(10)	Mn1−C5−N5	175.7(14)
N6−Mn2−N6_f	180.00		

a = 1−x,1−y,z; c =1/2+x,1/2−y,2−z; d =1/2−x,−1/2+y,2−z; f =1−x,1−y,2−z; h =x,y,2−z

Framework Stability: Thermogravimetric (TG) and Powder X-ray Diffraction (PXRD) Analysis.

Thermogravimetric analysis (TGA) and powder X-ray diffraction (PXRD) measurements at different temperatures were carried out to study the stability of the Compound **1**. TGA ofcompounds **1−1a** was performed in the temperature range of 30−700 °C under a N_2 atmosphere. The TGA profile of compound **1** (Fig S5) indicates a weight loss of 4.1% at 150 °C,

which corroborates the removal of four water molecules (cal. 5.3%). The second step was observed at 215°C with a weight loss of 24.8%, indicating the removal of all guest bipy and coordinated water molecules (cal.28.3%). The desolvated framework is stable up to 260 °C. The PXRD patterns of compounds **1** and its different forms are shown in Fig S3. Good correspondence of the different peak positions in the simulated and as-synthesized patterns suggests the phase purity of the as-synthesized compound. In case of **1a**, the similarity of the PXRD patterns between as-synthesized and heated samples indicates the structural integrity after the activation procedure, however broadening of some peaks suggests decrease in crystallinity after guest removal. The PXRD patterns of the rehydrated samples have not changed significantly even after exposing water vapor for 15 days, suggesting the framework is stable in the presence of water vapor.
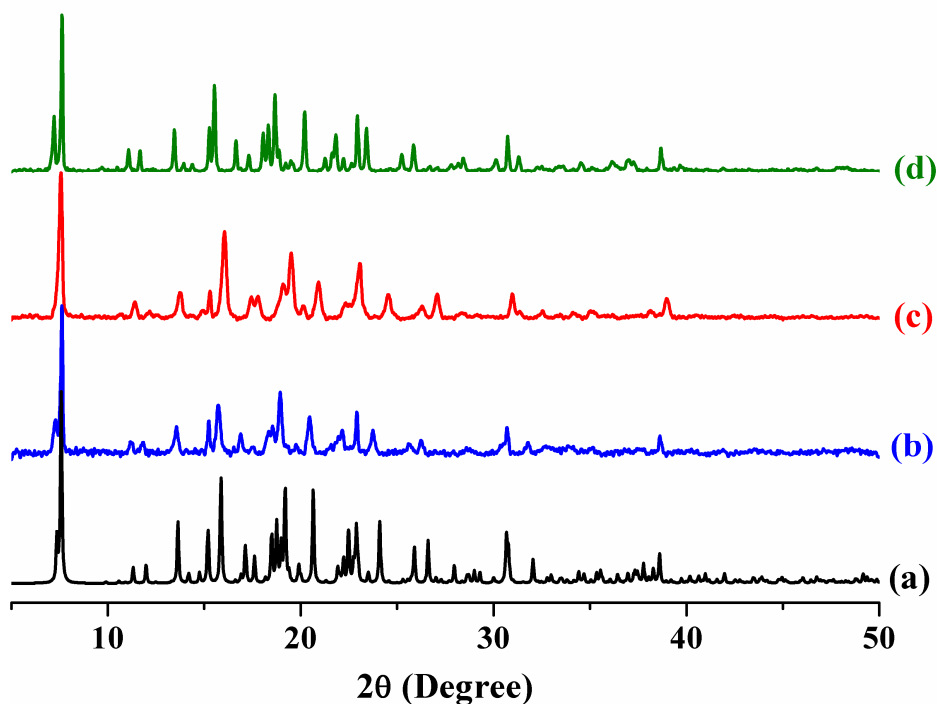

Fig.S3: PXRD patterns of compound **1** in different states: (a) simulated, (b) as-synthesized, (c) heated at 150 °C under vacuum. (d) Compound **1a** after exposing to the water vapour for 15 days.
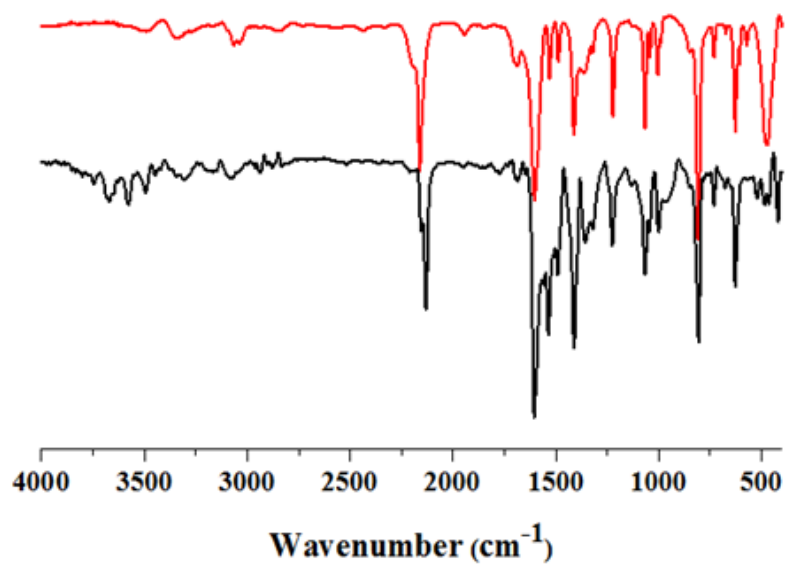
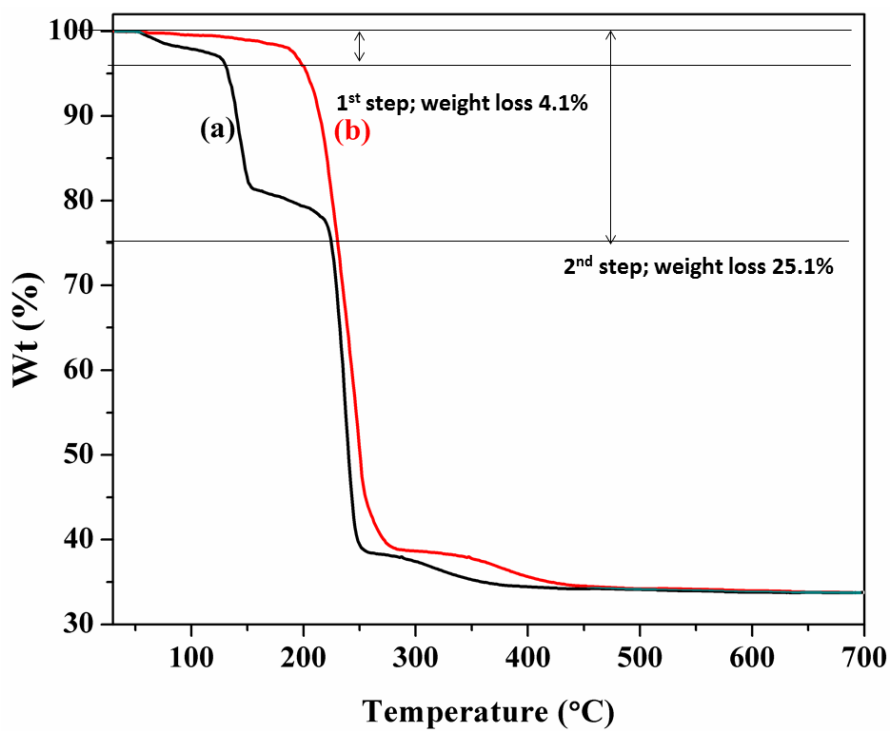***Fig. S4:*** IR spectra of **1** (black) and **1a** (red).

Fig. S5: TGA plots of compounds **1** and **1a** over the temperature range of 30 to 700 ℃ under N_2 atmosphere.

Analysis of Gas Adsorption Isotherms:

Sample preparation for the gas adsorption study:

N_2 (77 K), CO_2 (195 K,), C_2H_2 (273, 283 and 293 K), C_2H_4 (293 K) and C_2H_6 (293 K) adsorption studies were carried out with the desolvated sample, that is, **1a** by using an AUTOSORB IQ2 instrument. All the gases used for adsorption measurement are of scientific/research grade with 99.999% purity.The sample was prepared by heating compound **1** in QUANTACHROME sample cell at 120 °C under a reduced pressure ($< 10^{-1}$ Pa) for 72 hrs. During the heating period, the sublimed guest bipy molecules were deposited on the inner wall of the adsorption cell (Fig. S2). The activation procedure was continued by changing the sample cells time to time until there was no trace of guest bipy molecule. Dead volume was measured with helium gas. Adsorbent samples weighing around 100−150 mg were placed in the sample tube. The equilibrium time for every point of these measurements was set to 10 min with a tolerance value of 2. All operations were computer-controlled and automatic.
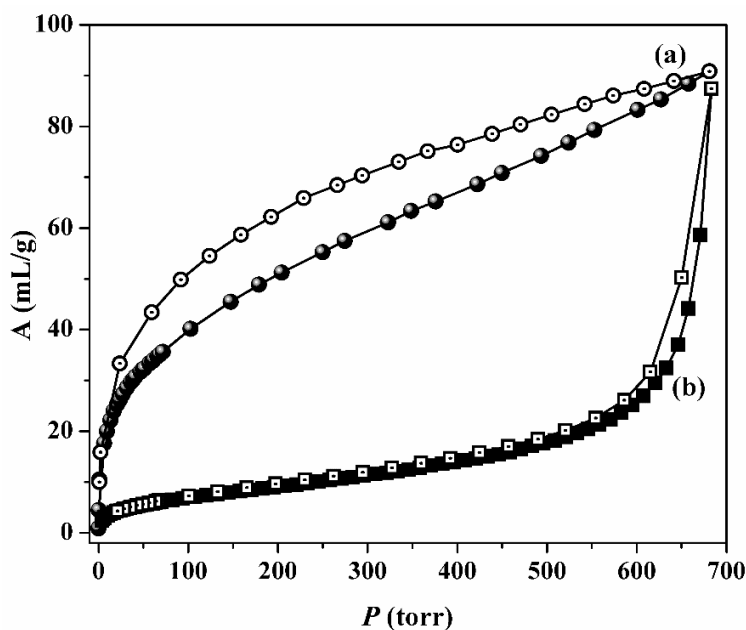

Fig.S6: CO_2 (a) and N_2 (b) adsorption isotherms of compound **1a** measured at 195 and 77 K respectively.
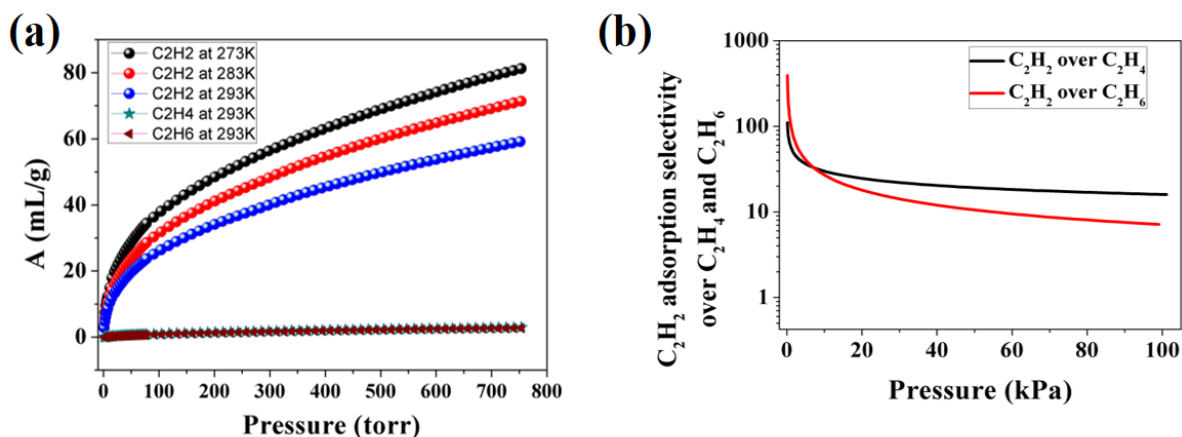
Fig. S7: (a) C₂H₂ (273, 283 and 293K), C₂H₄ (293 K) and C₂H₆ (293K) adsorption isotherms of Compound **1a**. (b) Predicted adsorption selectivity obtained by the calculation from IAST theory for C₂H₂ vs. C₂H₄ (black line) and C₂H₂ vs. C₂H₆ (red line) at 293 K

Heat of Adsorption (kJ mol⁻¹):

Virial Equation: We have used a virial type expression of the following type to fit the combined isotherms data collected at 273, 283 and 293 K.

$$\ln(P) = \ln(A) + \frac{1}{T}\sum_{i=0}^{m} a_i A^i + \sum_{i=0}^{n} b_i A^i \ldots\ldots\ldots(1)$$

Here, P is the pressure expressed in torr, A is the amount adsorbed in mmol/g, T is the temperature in K, a_i and b_i are virial coefficients, and m, n represent the number of coefficients required to adequately describe the isotherms. The value of m and n was gradually increased until the contribution of extra added a and b coefficients were negligible towards the overall final fit. The values of the virial coefficient a_i were taken to calculate the isosteric heat of adsorption using the following expression.

$$Q_{st} = -R \sum_{i=0}^{m} a_i A^i \ldots\ldots\ldots(2)$$

Q_{st} is the coverage dependent isoteric heat of adsorption and ***R*** is the universal gas constant.

The table inside the figure:

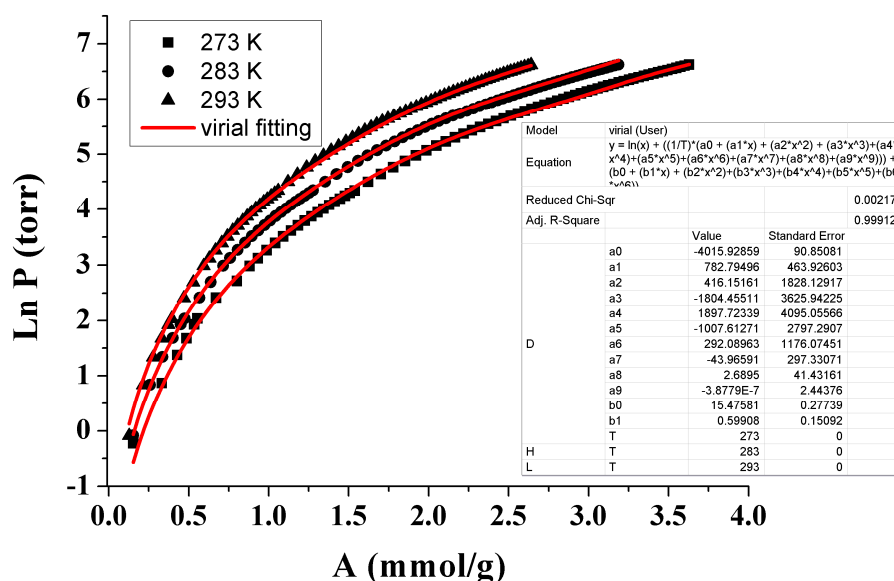| Model	virial (User)		
Equation	y = ln(x) + ((1/T)*(a0 + (a1*x) + (a2*x^2) + (a3*x^3)+(a4* x^4)+(a5*x^5)+(a6*x^6)+(a7*x^7)+(a8*x^8)+(a9*x^9))) + (b0 + (b1*x) + (b2*x^2)+(b3*x^3)+(b4*x^4)+(b5*x^5)+(b6 *x^6))		
Reduced Chi-Sqr			0.00217
Adj. R-Square			0.99912
		Value	Standard Error
	a0	-4015.92859	90.85081
	a1	782.79496	463.92603
	a2	416.15161	1828.12917
	a3	-1804.45511	3625.94225
	a4	1897.72339	4095.05566
	a5	-1007.61271	2797.2907
D	a6	292.08963	1176.07451
	a7	-43.96591	297.33071
	a8	2.6895	41.43161
	a9	-3.8779E-7	2.44376
	b0	15.47581	0.27739
	b1	0.59908	0.15092
	T	273	0
H	T	283	0
L	T	293	0

Fig. S8: C_2H_2 isotherms for activated compound **1** (**1a**) measured at 273 K (rectangle), 283 K (circle) and 293 K (triangle). Fitted curves (red solid lines), obtained from the virial-type expansion, were used for the Q_{st} estimation.
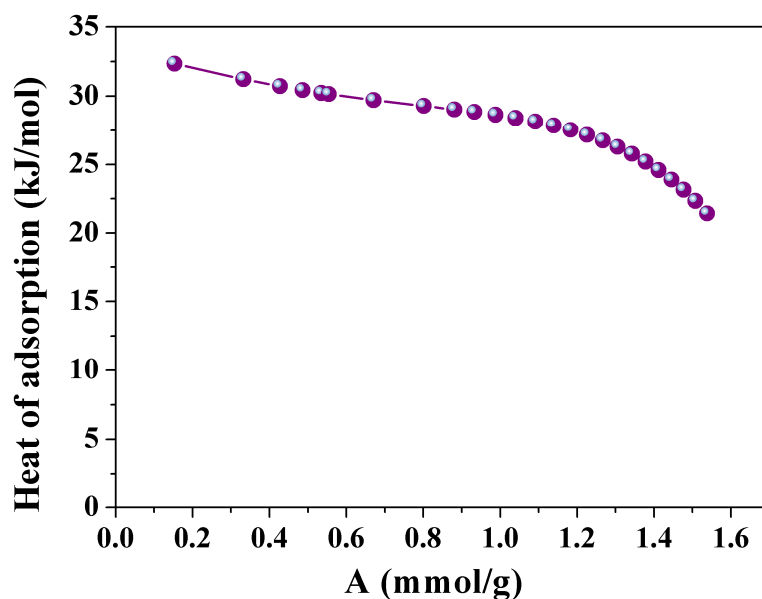

Fig. S9: Change of enthalpy of adsorption for C_2H_2 with the increase of loading for **1a** (calculation based on adsorption at 273, 283 and 293 K by using the virial equation).

IAST Selectivity:

The ideal adsorbed solution theory (IAST)[7] was used to predict the binary mixture adsorption of C_2H_2/C_2H_4 and C_2H_2/C_2H_6 from the experimental pure-gas isotherms. Previous reports have depicted that this method can predict the adsorption selectivity for mixture of isotherms in nano-porous materials, including metal-organic frameworks.[8] The single-component isotherms were fit to a single-site Langmuir-Freundlich equation[4] (equation 5). The IAST assumes that the adsorbed phase is a two-dimensional solution in equilibrium with the bulk phase.[7a] For binary adsorption of A and B, the IAST requires these two equations to be followed:

$$yP_t = xP_a \ldots\ldots\ldots\ldots\ldots\ldots\ldots\ldots\ldots.(3)$$
$$(1-y)P_t = (1-x)P_b \ldots\ldots\ldots\ldots\ldots.(4)$$

Where x and y denote the molar fraction of A in the adsorbed phaseand the molar fraction of A in the bulk phase, respectively. P_t is the total gas pressure; P_a and P_b are the pressure of component A and B at the same spreading pressure as that of the mixture, respectively. The equation used for the fitting the single component gas mixture is as follows.

$$Y = Y_0 \left(ln \frac{BP^n}{(1+BP^n)}\right) \ldots\ldots\ldots\ldots\ldots\ldots.(5)$$

Furthermore, the molar fraction of A in the adsorbed phase can be obtained from the following equation:

$$Y_{0,a} \ln\left(1 + \frac{B_a P_t^{n1} y}{x}\right) - Y_{0,b} \ln\left(1 + \frac{B_b P_t^{n2}(1-y)}{(1-x)}\right) = 0 \ldots\ldots\ldots.(6)$$

Where $Y_{0,a}$, B_a and $n1$ are the Langmuir-Freundlich fitting parameters of adsorption equilibrium of pure A, $Y_{0,b}$, B_b and $n2$ are Langmuir-Freundlich parameters of adsorption equilibrium of pure B. The unknown x in Eq. (6) has been solved by Matlab (Version 7.8 (R2009a), The MathWorks, Inc.) for fixed P_t and y values.

Then calculated the predicted adsorption selectivity, which is defined as

$$S = \left(\dfrac{\dfrac{x_1}{y_1}}{\dfrac{x_2}{y_2}}\right) \ldots\ldots\ldots\ldots\ldots..(7)$$

Where x_i and y_i are the mole fractions of component i (i = 1, 2; A, B) in the adsorbed and bulk phases, respectively. The IAST calculations were carried out for equimolar gas-phase mixtures.

Column Breakthrough Experiment:

The performance of **1a** in the actual adsorption-based separation and purification process of acetylene from C_2H_2/C_2H_4 mixtures containing 1% acetylene was examined through experimental column breakthrough (Fig. S10) in which a C_2H_2/C_2H_4 (1:99, v/v) mixture was flowed through a packed column of **1a** with a total flow rate of 2.2 mL min^{-1} at 293 K. C_2H_4 molecules were detected at the output of the column after 1.2 min of starting the gas flow through **1a** whereas no trace of C_2H_2 was found upto 19.1 min. After that, C_2H_2 molecules slowly started releasing from the outlet which was saturated after 45 min. The efficient purification of C_2H_4 from the gas mixture has been successfully achieved with a total C_2H_2 retention time of 17.9 min.
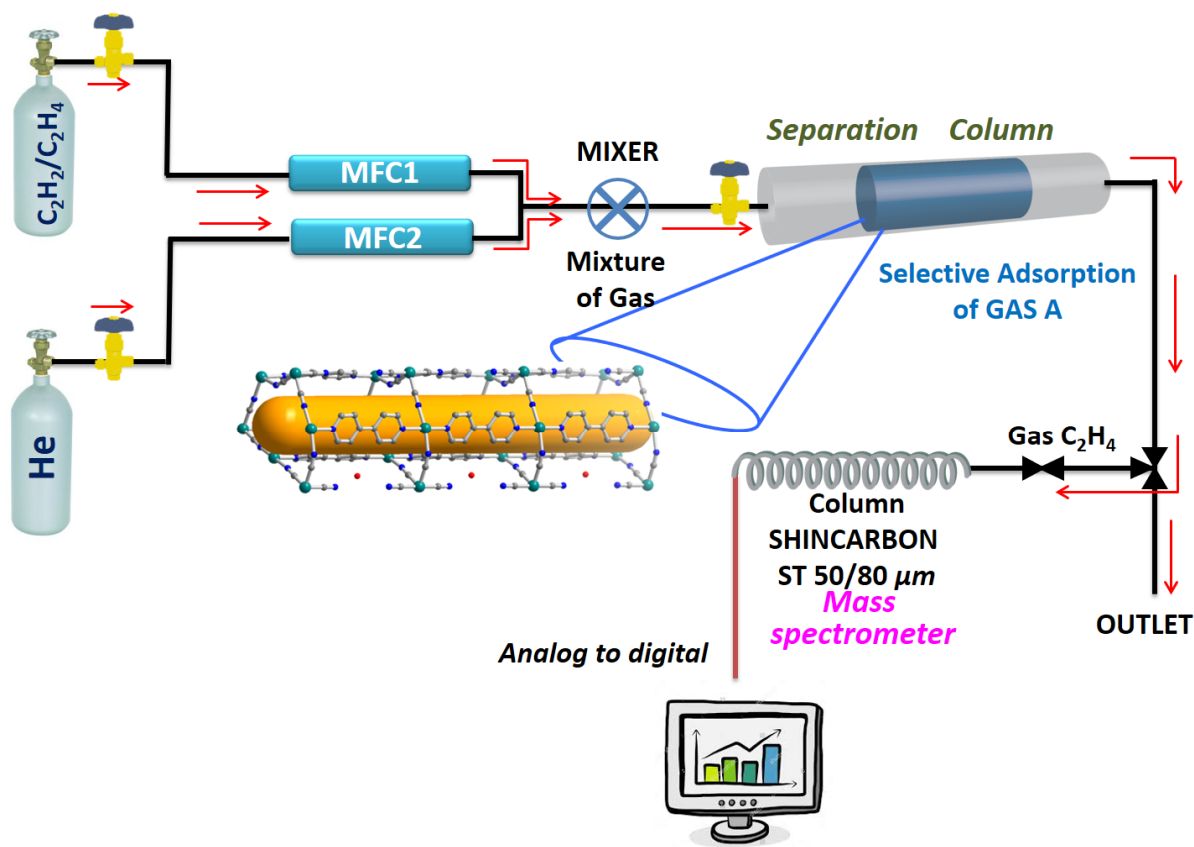
Fig. S10: Schematic representationof instrument set up used for C_2H_2/C_2H_4 break-through measurement in**1a** at room temperature.

Computational Details

To obtain a microscopic understanding of the difference in the adsorption of C_2H_2, C_2H_4, and C_2H_6in MOF, we employed periodic density functional theory (periodic-DFT) based calculations. To identify the optimal location of gas molecules inside the MOF, periodic-DFT calculations were carried out using QUICKSTEP module in CP2K software.[9]All valence electrons were treated in a mixed basis set with an energy cutoff of 400 Ry. The short-range version of the double-ζ single polarization basis set was used. The effect of core electrons and nuclei was considered by using pseudopotentials of Goedecker-Teter-Hutter (GTH).[10] The exchange and correlation interaction between electrons was treated with the exchange functional (xGGA) PW86x.[11] van der Waals interactions between the gas and the framework are imperative, their effects were accounted for by employing empirical corrections developed by

Grimme (DFT-D3)[12] and non-local van der Waals density functional kernel, vdW-DF2 functional (LMKLL).[13] This is used to calculate the cell volume and binding energy. The simulation cell consisted $1 \times 1 \times 2$ unit cells. Gas phase density functional calculation were also performed using B3LYP-D3/def2-QZVP level of theory[14] to get the binding energy using Orca 2.9.1 software package.[15] The binding energy of gas to **1a** was calculated as

$$\Delta E = E_{(MOF+gas)} - E_{(MOF)} - E_{(gas)} \qquad (8)$$

Here $E_{(MOF+gas)}$ is the energy of the MOF with gas molecule, $E_{(MOF)}$ is the energy of the MOF, and $E_{(gas)}$ is the energy of the isolated gas molecule. The energy of an isolated gas molecule was calculated in the same simulation box size as that of the MOF. All structures were visualizing using VMD,[16] Mercury,[17] and GaussView[18]. Alongside periodic DFT calculations, accurate gas phase quantum mechanical calculations were performed to obtain the binding energy where **1a** was represented by replacing the coordinatively saturated metals by hydrogen atoms and 4,4′-bipyridine by pyridine alone. The binding energy obtained from the gas phase calculation at B3LYP-D3/def2-QZVP level of theory is 65.31 kJmol^{-1}. These results are also corroborated by the binding energy obtained from the periodic DFT calculations.
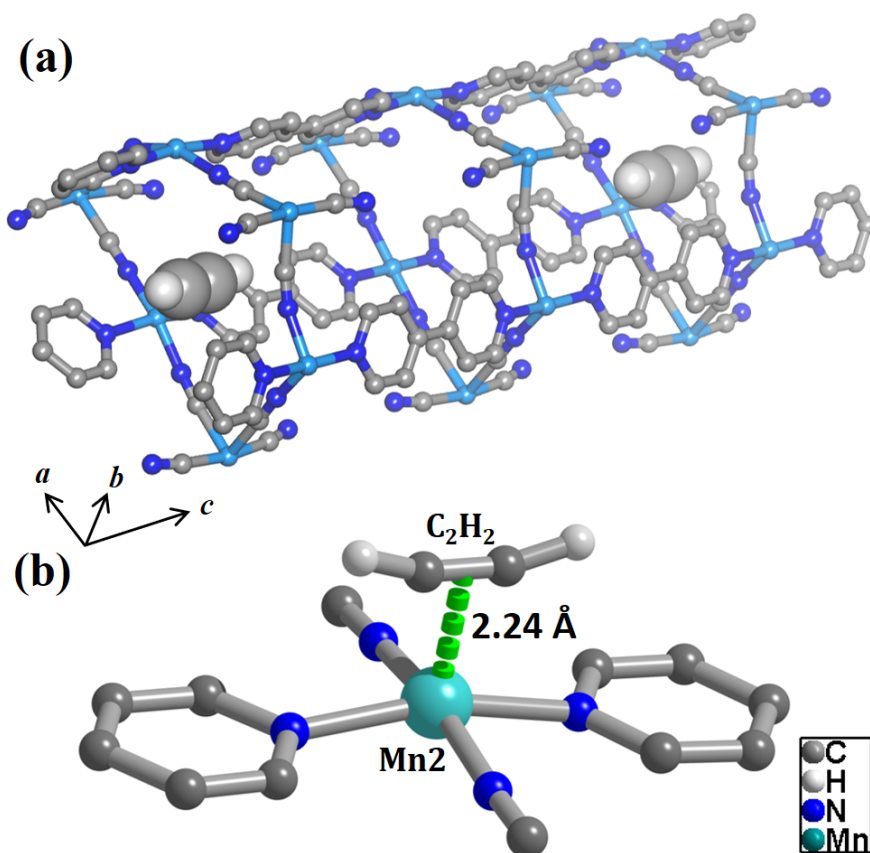
Fig. S11: (a) The optimized position of C_2H_2 molecules in the geometry optimized structure of **1a**. (b) Detail view of the interaction of C_2H_2 with four coordinated Mn^{II} center.

Supporting Information References

1. S. V. a. SMART (V 5.628), XPREP, SHELXTL; Bruker AXS Inc. Madison, Wisconsin, USA, 2004.

2. G. M. Sheldrick, *SADABS, Empirical Absorption Correction Program, University of Göttingen, Göttingen*, 1997.

3. A. Altomare, G. Cascarano, C. Giacovazzo and A. Guagliardi, *J. Appl. Crystallogr.*, 1993, **26**, 343-350.

4.   G. M. Sheldrick, *SHELXL 97, Program for the Solution of Crystal Structure, University of Göttingen, Germany*, 1997.

5.   A. Spek, *J. Appl. Crystallogr.*, 2003, **36**, 7-13.

6.   L. Farrugia, *J. Appl. Crystallogr.*, 1999, **32**, 837-838.

7.   (a) A. L. Myers and J. M. Prausnitz, *AlChE J.*, 1965, **11**, 121-127;(b) Y.-S. Bae, K. L. Mulfort, H. Frost, P. Ryan, S. Punnathanam, L. J. Broadbelt, J. T. Hupp and R. Q. Snurr, *Langmuir*, 2008, **24**, 8592-8598;(c) Y.-L. Huang, Y.-N. Gong, L. Jiang and T.-B. Lu, *Chem. Commun.*, 2013, **49**, 1753-1755;(d) J. Qian, F. Jiang, D. Yuan, M. Wu, S. Zhang, L. Zhang and M. Hong, *Chem. Commun.*, 2012, **48**, 9696-9698.

8.   (a) R. Babarao, Z. Hu, J. Jiang, S. Chempath and S. I. Sandler, *Langmuir*, 2006, **23**, 659-666;(b) B. Liu and B. Smit, *Langmuir*, 2009, **25**, 5918-5926.

9.   J. VandeVondele, M. Krack, F. Mohamed, M. Parrinello, T. Chassaing and J. Hutter, *Comput. Phys. Commun.*, 2005, **167**, 103-128.

10.   M. Elstner, D. Porezag, G. Jungnickel, J. Elsner, M. Haugk, T. Frauenheim, S. Suhai and G. Seifert, *Physical Review B*, 1998, **58**, 7260-7268.

11.   É. D. Murray, K. Lee and D. C. Langreth, *Journal of Chemical Theory and Computation*, 2009, **5**, 2754-2762.

12.   S. Grimme, J. Antony, S. Ehrlich and H. Krieg, *J. Chem. Phys.*, 2010, **132**, 154104.

13.   K. Lee, É. D. Murray, L. Kong, B. I. Lundqvist and D. C. Langreth, *Physical Review B*, 2010, **82**, 081101.

14.   (a) F. Weigend and R. Ahlrichs, *PCCP*, 2005, **7**, 3297-3305;(b) A. D. Becke, *J. Chem. Phys.*, 1993, **98**, 5648-5652.

15.   *Orca 2.9.1, developed by Frank Neese, Max Planck Institute for Bioinorganic Chemistry, Mülheim/Ruhr, Germany*.

16.   W. Humphrey, A. Dalke and K. Schulten, *J. Mol. Graphics*, 1996, **14**, 33-38.

17.   C. F. Macrae, P. R. Edgington, P. McCabe, E. Pidcock, G. P. Shields, R. Taylor, M. Towler and J. van de Streek, *J. Appl. Crystallogr.*, 2006, **39**, 453-457.

18.   R. Dennington, T. Keith and J. Millam, *GaussView Version 5 Semichem Inc. Shawnee Mission KS*, 2009.